Atmos. Chem. Phys. Discuss., 9, 183–223, 2009
www.atmos-chem-phys-discuss.net/9/183/2009/

Atmospheric Chemistry and Physics Discussions

This discussion paper is/has been under review for the journal *Atmospheric Chemistry and Physics (ACP)*. Please refer to the corresponding final paper in *ACP* if available.

Observations of high rates of NO_2 – HONO conversion in the nocturnal atmospheric boundary layer in Kathmandu, Nepal

Y. Yu[1,*], B. Galle[1], E. Hodson[2,], A. Panday[2,***], R. Prinn[2], and S. Wang[3]**

[1]Optical Remote Sensing, Radio and Space Science, Chalmers University, 41296 Gothenburg, Sweden
[2]Department of Earth, Atmospheric, and Planetary Sciences, Massachusetts Institute of Technology, Cambridge, MA 02139, USA
[3]Jet Propulsion Laboratory, Pasadena, CA 91109, USA
[*]now at: Department of Chemistry, UC Irvine, Irvine, CA 92697-2025, USA
[**]now at: Ecological Process Modelling Unit, Swiss Federal Institute for Forest, Snow and Landscape Research, Birmensdorf, 8903, Switzerland
[***]now at: Atmospheric and Oceanic program, Princeton University, Princeton, NJ 08544, USA

Received: 7 October 2008 – Accepted: 13 November 2008 – Published: 6 January 2009

Correspondence to: Y. Yu (yongy@uci.edu)

Published by Copernicus Publications on behalf of the European Geosciences Union.

Abstract

Nitrous acid (HONO) plays a significant role in the atmosphere, especially in the polluted troposphere. Its photolysis after sunrise is an important source of hydroxyl free radicals (OH). Measurements of nitrous acid and other pollutants were carried out in the Kathmandu urban atmosphere during January–February 2003, contributing to the sparse knowledge of nitrous acid in South Asia. The results showed average nocturnal levels of HONO (1.7±0.8 ppbv), NO_2 (17.9±10.2 ppbv), and PM_{10} (0.18±0.11 mg m^{-3}) in urban air in Kathmandu. Surprisingly high ratios of chemically formed secondary [HONO] to [NO_2] (up to 30%) were found, which indicates unexpectedly efficient chemical conversion of NO_2 to HONO in Kathmandu. The ratios of [HONO]/[NO_2] at nights are much higher than previously reported values from measurements in urban air in Europe, North America and Asia. The influence of aerosol plumes, relative humidity, aerosol surface and ground reactive surface, temperature on NO_2-HONO chemical conversion were discussed. The high humidity, strong and low inversion layer at night, and serious aerosol pollution burden may explain the particularly efficient conversion of NO_2 to HONO.

1 Introduction

Atmospheric nitrous acid (HONO) has been studied for a long time and at a wide range of locations. It can be an important source of hydroxyl free radical (OH) in the atmosphere, especially in the morning (Lammel and Cape, 1996; Harrison et al., 1996). Despite nitrous acid's importance, its formation mechanism remains unclear after several decades of studies. Further investigation of the source of nitrous acid in the atmosphere is important to understand atmospheric chemistry processes.

One source of atmospheric HONO is the gas phase reaction from NO and OH (Seinfeld and Pandis, 1998; Lammel, 1999; Kleffmann, 2007). However, the gaseous phase reactions (including NO with OH free radicals and NO_2 with peroxy or alkoxy

ACPD

9, 183–223, 2009

radicals – Stockwell and Calvert, 1983) are too slow to explain the atmospheric HONO concentration. Direct emission from combustion engines is another source of HONO in the atmosphere (Kurtenbach et al., 2001; Kirchstetter et al., 1996; Wormhoudt et al., 2007; Geiger et al., 2002). A ratio of HONO to total NO_x ($NO+NO_2$) ranging from 0.3%–0.8% has been observed in the direct emission from the vehicle engines. However, observations of HONO-to-NO_2 ratios of a few percent in a wide range of urban atmospheres suggest that direct emission from combustion engines probably is not a major source of HONO.

Heterogeneous formation (Reactions 1–3) is believed to be a key source of HONO, but the mechanism is not well understood.

$$NO_{2(ads)} + NO_{2(ads)} + H_2O_{(surface)} \rightarrow HNO_{2(g)} + HNO_{3(aq)} \quad \text{(R1)}$$

$$NO_2 + NO + H_2O_{(surface)} \rightarrow 2HNO_2 \quad \text{(R2)}$$

$$NO_{2(g)} + HC_{red} \rightarrow HONO_{(g)} + HC_{ox} \quad \text{(R3)}$$

Reaction (1) is one of the most prominent processes for HONO heterogeneous formation (Finlayson-Pitts et al., 2003). Past research on the mechanism of HONO heterogeneous reactions points to the importance of reaction surfaces and indicates that the production efficiency of HONO depends upon the amount of water absorbed by surfaces (Finlayson-Pitts et al., 2003; Kurtenbach et al., 2001; Grassian, 2001, 2002). Nitrous acid can be formed through Reaction (1) on the surface of aerosols and ground (Trick, 2004; Harrison and Kitto, 1994; Andres-Hernandez et al., 1996; Reisinger, 2000; Wang et al., 2003; Notholt et al., 1992a).

Recently, reactions of NO_2 on the soot (Reaction 3) has been shown to be a source of HONO in the atmosphere (Aubin and Abbatt, 2007; Alcala-Jornod et al., 2000; Nienow and Roberts, 2006; Ammann et al., 1998; Gerecke et al., 1998; Longfellow et al., 1999; Arens et al., 2001; Al-Abadleh and Grassian, 2000; Aumont et al., 1999; Grassian, 2001, 2002; Karagulian and Rossi, 2007). Soot (or back carbon) aerosols often have a loading of 1.5 to 20 $\mu g\, m^{-3}$ in the urban air from anthropogenic sources such as fossil fuel combustions (IPCC, 2001). The fractal and porous surface of soot make a large

contribution to the total reactive aerosol surface even when soot may have a relatively small contribution to the total aerosol mass. Studies using black carbon and soot as a substrate have demonstrated the reactive uptake of NO_2 and formation of NO and HONO (Aubin and Abbatt, 2007; Kleffmann, 2007).

Atmospheric measurements, laboratory studies and model calculations have shown the enhanced formation of HONO during the daytime (Stemmler et al., 2007; George et al., 2005; Gustafsson et al., 2006; Beine et al., 2006; Bejan et al., 2006; Rohrer et al., 2005; Liao et al., 2006a; Zhou et al., 2001; Honrath et al., 2002; Domine and Shepson, 2002; Akimoto et al., 1987; Kleffmann, 2007; Arens et al., 2002). It has also been shown that NO_2 can be efficiently reduced to form HONO under the UV light on the surface of Ti_2O, humid acid, phenol, nitro-phenol and other organic compounds (Reaction 4) (Kleffmann, 2007; Stemmler et al., 2007; Stemmler et al., 2006; George et al., 2005; Lahoutifard et al., 2002; Gustafsson et al., 2006; Bejan et al., 2006).

$$NO_{2(g)} + \text{photo-activated aerosol surface} \rightarrow HONO_{(g)} \quad \text{(R4)}$$

Nitrous acid formed in homogenous and heterogeneous reactions is released to the gas phase and can be accumulated during the night. Photolysis of accumulated HONO in the atmosphere after sunrise provides a pulse of OH free radicals and strongly influences the atmospheric chemistry processes. Field measurements of HONO and its precursor NO_2 at locations with various aerosol load, aerosol composition, and relative humidity are thus essential for improving our understanding of the HONO formation mechanism.

Gaseous HONO in ambient air was measured for the first time by Perner and Platt (Perner and Platt, 1979) using differential optical absorption spectroscopy (DOAS). Besides the DOAS technique, a variety of other methods/instruments have been developed for the detection of HONO in the atmosphere with high sensitivity and good time resolution (Liao et al., 2006a, b; Takenaka et al., 2004; Trebs et al., 2004; Kleffmann et al., 2002; Huang et al., 2002; Vecera and Dasgupta, 1991; Heland et al., 2001; Zhou et al., 2002, 2007). Measurements of HONO in the atmosphere have been carried out

in many areas of Europe and the United States. However, the knowledge of HONO sources, sinks, and concentrations is almost nonexistent in South Asia. Due to the different source strengths, aerosol burdens, and the composition of aerosol and ground surfaces, the HONO chemistry in South Asia is expected to have different features than what is found in Europe or the North America. For example, the average aerosol burden in the atmosphere of Kathmandu is much higher than in European and US cities (Sharma et al., 2002; Sharma, 1997; Yu et al., 2008a; Giri et al., 2006) in the winter. Moreover, strong nocturnal inversion layer (Kondo et al., 2002; Regmi et al., 2003; Panday, 2006) and low mixing layer height keeps pollutants close to the ground providing a large reactive ground surface for HONO formation. The high aerosol concentrations and the strong inversion layer might play an important role in the heterogeneous formation of HONO.

In this study, we present measurements of HONO and NO_2 using long path DOAS that were carried out in Kathmandu, Nepal, over several weeks in 2003. As far as we are aware, this is the first time that HONO's behavior in the nocturnal atmosphere, and its relation to NO_2, has been studied anywhere in South Asia. Our observations indicate the particular HONO chemical formation processes taking place in the Kathmandu atmosphere.

2 Experimental section

2.1 Location and instruments

We carried out a field campaign in Kathmandu in winter 2003, investigating air quality and atmospheric chemistry processes. NO_x (NO, NO_2), SO_2, O_3, HONO, HCHO, PM_{10}, and meteorological data were measured during this period.

Home-made long-path DOAS (Chalmers University) was used to measure HONO and NO_2 with the time resolution around 5–10 min at the Kathmandu urban area. DOAS measurements were carried from 10 January to 11 February 2003. The mea-

ACPD
9, 183–223, 2009

surement site (27°43.2190′ N, 85°21.417′ E) was about 2 km east of the Kathmandu Ringroad, along the main road from Kathmandu to Sankhu (Fig. 1). A DOAS telescope and other instruments (NO_x analyzer, O_3 monitor, PM_{10}/TSP aerosol monitor) were installed on the 5th floor of a hotel (15 m above ground). DOAS retro-reflectors were mounted at the top of a 7-story building, 25 m above ground and 957 m away from the DOAS telescope, giving a DOAS light path of 1914 m. Low buildings, roads, and some bare fields were under the light path. An automated weather station which measured temperature, wind speed, wind direction, relative humidity, dew point temperature, and solar radiation was installed on the roof of the hotel (22 m above ground) near the DOAS telescope and other instruments. Details of the DOAS instrument and of the experimental sites have been described in earlier papers (Yu et al., 2004, 2008a).

2.2 Retrieval method of aerosol parameters

To investigate the importance of aerosols in the HONO formation processes, measurements of aerosol parameters such as the aerosol surface density are required along with the ambient concentration of HONO and NO_2. Box and Lo (1976) had developed a simple inversion method to calculate the approximate aerosol size distribution from light attenuation. This has been further applied to calculate other aerosol parameters such as the surface density and the volume using DOAS measurements (Notholt et al., 1991, 1992a, b; Notholt and Raes, 1990; Flentje et al., 1997; Reisinger, 2000).

Light transmission measurements through the atmosphere can yield bulk aerosol parameters such as diameters, number density, total surface, and total volume of particles (Livingston and Russell, 1989). Here we used the DOAS system in Kathmandu to perform the light transmission measurements and to measure the aerosol parameters and trace gas concentrations simultaneously over the same air volume.

The spectra were recorded in the 250–390 nm range. The range 330 nm to 390 nm was used to retrieve concentrations of HONO, NO_2 and aerosol parameters simultaneously. A background spectrum was recorded over a 1 m optical path using retroreflectors. Giving the concentrations of all gases provided by the DOAS spectra retrieval

processes (SO_2, O_3, NO_2, HONO, and HCHO), the optical depth (τ) for different wavelengths can be calculated according to Eq. (1).

$$\tau(\lambda) = -\ln\left(\frac{I(\lambda)}{I_0(\lambda)}\right) \quad (1)$$

Here, $I(\lambda)$ is the light intensity at the corresponding path length and $I_0(\lambda)$ is the background light intensity at 1 m path length. Inversion of the optical depth was performed using a look-up table (Box and Lo, 1976). This assumes an exponential wavelength-dependent function $\tau_{exp}(\lambda)$ for optical depth:

$$\tau_{exp}(\lambda) = \beta \cdot e^{-\alpha \cdot \lambda} - k \quad (2)$$

where $\tau_{exp}(\lambda)$ is the optical depth with, α and β are the fitting parameters, and k is the offset constant.

This formula (2) is used to fit to the experimental values in the spectral region 330–390 nm. The offset k must be considered because of instrument factors such as the reflecting ratio of retroreflectors. Using α, β and the pre-calculated tables of Box and Lo (1976) values for a and b can be obtained to be applied in Deirmendjian's particles size distribution $n(r)$ (Box and Lo, 1976; Notholt and Raes, 1990; Notholt et al., 1992b; Notholt et al., 1991):

$$n(r) = \frac{1}{2} \cdot a \cdot b^3 \cdot r^2 \cdot e^{-b \cdot r} \quad (3)$$

where r is the particle radius and where the constants (a and b) are specified for the different particles types.

By using same method as Notholt et al. (1992a) but with a narrower spectral range, we have carried out the calculation of aerosol size distribution and further obtained the total number, surface density and the volume of aerosols in time intervals of 5–10 min.

Our light attenuation retrieval processes give a large uncertainty of aerosol parameters. Errors in this method have been extensively discussed by others (Andres-Hernandez et al., 1996; Notholt et al., 1992a; Notholt and Raes, 1990; Box and Lo, 1976). The total error of our results was estimated to be 55%. It comes from:

1. The unknown refractive index of the aerosols (we have tested different indices from 1.33 to 1.70. Trends with different indices are similar but with floating values) could contribute an uncertainty as large as 50% (Box and Lo, 1976);

2. The relatively narrow spectral range compared to the application by Notholt et al. (1992a) gave 20% uncertainty as reported by Reisinger (2000);

3. The deviation between the true aerosol size distribution and the calculated results by the model (Deirmendjian's particles size distribution) could introduce additional uncertainty;

4. Lamp intensity and DOAS mechanical stability can provide sufficient information during a time period of a few weeks but with 10% error (Andres-Hernandez et al., 1996; Notholt et al., 1992a).

With such limitations, the results of aerosol parameters are only approximations of the true aerosol situation. Nevertheless, the retrieval results of aerosol surface and volume (assuming a refractive index n=1.5 – Yu et al., 2008b) agree well with the trends seen in our PM_{10} data (Fig. 2), which confirms the reliability of our calculated aerosol parameters.

The aerosol mass in this study could be calculated by the urban aerosol density ($\sim 1.4 \pm 0.5\,g\,cm^{-3}$ – Pitz et al., 2003) and aerosol volume ($\sim 1 \times 10^2\,\mu m^3\,cm^{-3}$, 12:00 a.m.–04:00 a.m. in Kathmandu atmosphere in Fig. 2). The average aerosol mass at midnight of Kathmandu air equals to $140 \pm 50\,\mu g\,m^{-3}$. However, light attenuation only gives the aerosol information (aerosol diameters, surface and volume) for fine particles with diameters smaller than 1 µm. Assuming a PM_1/PM_{10} mass ratio of 50% in urban air (Vallius et al., 2000; Ehrlich et al., 2007; Ariola et al., 2006; Spindler et al., 2004; Labban et al., 2004; Li and Lin, 2002; Gomiscek et al., 2004; Liu et al., 2004), the calculated aerosol mass by light attenuation is in agreement with our measured PM_{10} values.

3 Results and discussion

3.1 Time series of HONO, other pollutants and meteorological data

Continuous measurements were carried out during January and February 2003. Figure 3 shows, as an example from our one-month observation period, the behavior of HONO, NO_x, [HONO]/[NO_2], PM_{10}, and meteorological parameters (radiation, wind speed and wind direction). NO_2 and HONO measurements by the long path DOAS show gaps every morning and on some evenings due to heavy fog and smog.

The concentration of NO had two peaks (with values as high as 60 ppb) at 7–8 a.m. and 7–8 p.m., respectively, and remained low (a few ppb except for short duration plumes) at night. As our campaign was at a time of considerable political instability in Nepal, with frequent vehicle searches at night, night-time driving was quite low and thus the sources of NO were limited. Peaks in NO_2 appeared concurrently with the two NO peaks at 7–8 a.m. and 7–8 p.m.. NO_2 values were around 10–20 ppb at night, and started to increase again around 3–4 a.m. HONO concentrations climbed to several ppb after sunset and then decreased to around 1–1.5 ppb. It increased again after 3 a.m. PM_{10} shows elevated values (up to 1 mg m^{-3}) during the morning and evening. The diurnal variation of the observed wind pattern shows a long calm period from sunset (~6 p.m.) until around 10 a.m. each day. The morning and evening peaks in NO_x and PM_{10} did not correspond to rush hour alone. In particular, the evening peaks started after the rush hour. The timing of pollutant peaks in Kathmandu is determined by the valley's ventilation pattern (Panday, 2006). The correlation of HONO with NO_2 and PM_{10} (especially after sunset) in Fig. 3 indicates either the same emission source, or chemical conversion of NO_2 to HONO associated with aerosols. The HONO formation mechanism will be discussed in later sections.

Table 1 shows several pollutants measured in Kathmandu urban air. Elevated mixing ratios of HONO (up to ~7.5 ppbv) were observed during the whole measurement period. The elevated HONO concentrations in the presence of high [NO], [NO_2] and PM_{10} values right after sunset appear to be the result of several processes:

ACPD
9, 183–223, 2009

1. direct emission at evening rush hours;
2. decrease of boundary layer height after sunset;
3. insufficient dispersion of polluted air mass due to reduced wind speed;
4. the ceasing of photolysis of NO_2 and HONO after sunset.

Table 2 lists HONO measurements in Asia. Elevated atmospheric HONO concentrations have been detected in Asian cities, suggesting that HONO might be an important source for the OH free radical budget in these places.

3.2 High atmospheric [HONO]/[NO_2] values in Kathmandu at night

In many field studies, the value of [HONO]/[NO_2] is used as an index to estimate the efficiency of heterogeneous NO_2-HONO conversion because it is less influenced by transport processes than individual concentrations. Figure 3 shows that, in Kathmandu, [HONO]/[NO_2] climbed after sunset and reached its highest point around 2–3 a.m.. The highest [HONO]/[NO_2] values during 3–7 February were from 15% to 28% between 0:00 and 03:00 a.m. The diurnally repeating trends of [NO_x], [HONO] and [HONO]/[NO_2] are most likely due to diurnally repeating wind profiles, emission sources, boundary layer dynamics and chemical processes. During rush hours and other plume events (around 7, 8, and 9 p.m.), [HONO] followed the same pattern as [NO_2] (Fig. 3). However, during those times a lower [HONO]/[NO_2] value (compared to later higher value) was observed, similar to the observation at Houston (Stutz et al., 2004). It is likely that conversion of NO_2 to HONO in relatively freshly polluted air has not proceeded as far as in the aged air in this period.

A scatter plot of [HONO] and [NO_2] for nocturnal data is shown in Fig. 4. The regression coefficient, maximum and minimum ratio of [HONO] to [NO_2] were 0.081, 0.30 and 0.008, respectively. The maximum [HONO]/[NO_2] ratio (30%) found in our observation is, to our knowledge, the highest reported atmospheric HONO to NO_2 ratio in the world. The high ratios of [HONO] to [NO_2] indicate either high HONO direct

emissions, or efficient NO_2 to HONO chemical conversion in the nocturnal Kathmandu urban atmosphere.

It is necessary to separate HONO formed by chemical reactions from the direct emissions (mainly from vehicles, the industrial combustion process contribution is not clear). No previous study has reported the ratio of [HONO] to [NO_x] in emissions from Kathmandu. The highest reported average emission ratio was (0.8±0.1)% anywhere in the literature (Kurtenbach et al., 2001). Based on the observation of HONO, NO_x and [HONO]/[NO_2] in this study, it appears that direct emission was not the major source of HONO in Kathmandu urban air: First, the [HONO] to [NO_2] ratio was low (around a few %) after sunset at a time when there were high NO_x concentrations. Second, NO_x concentrations were low in the middle night, ruling out the possibility of direct emission as the major source of HONO. Third, as we see in Fig. 4, the minimum value of [HONO]/[NO_2] was ~0.8%; indicating the maximum contribution of HONO direct emission.

The high value of [HONO]/[NO_2] (upto 20% during most nights, exceeding 25% during some nights, and reaching a maximum of 30% during one night) is thus mostly from secondary HONO. This maximum ratio of 30% is substantially higher than the previously observed ratios at other urban and suburban sites in Europe, North America and Asia (i.e., 1–12% reported by Lammel and Cape, 1996, 19% reported by Wang et al., 2003 during dust storms, and 1–13% around Asia – Qin et al., 2006; Park et al., 2004; Hao et al., 2006).

3.3 Additional NO_2 – HONO conversion during the pollution plumes

The continuous increasing [HONO]/[NO_2] ratio reaches ~15% from sunset to middle night (0 a.m.) on 3 February 2003 (Fig. 3). Figure 5 shows a close look at [HONO]/[NO_2], NO_x and PM_{10}, between 00:30 and 3:30 a.m. on 4 February 2003. It shows the unusual behavior of [HONO]/[NO_2] in more detail. Several small plume events (A–D in Fig. 5) from 1–3 a.m. (indicated by PM_{10} spikes and slightly increased [NO_2]) showed an interesting phenomenon: the [HONO] increased while [NO_2] de-

creased after the PM_{10} spike, and [HONO]/[NO_2] dropped at the onsets of plumes (right before the PM_{10} spike) and then increased drastically after the PM_{10} spike to ~25% (22%–27%) with several minutes delay. It shows that highly efficient conversion of NO_2 to HONO took place in plumes.

Recently, many researchers (Aubin and Abbatt, 2007; Alcala-Jornod et al., 2000; Nienow and Roberts, 2006; Ammann et al., 1998; Gerecke et al., 1998; Longfellow et al., 1999; Arens et al., 2001; Al-Abadleh and Grassian, 2000; Aumont et al., 1999; Grassian, 2001, 2002; Karagulian and Rossi, 2007) have reported the fast conversion of NO_2 on fresh soot surface to form HONO. They also report that the soot surface appears to deactivate with time. Although aerosol chemical properties in the Kathmandu urban area were not provided by our measurements, there are some literature reports as well as plenty reports in local newspapers to confirm that large amounts of soot exist in the winter Kathmandu urban air. Some researchers have attributed the dark haze over Kathmandu valley to the presence of soot particles as major pollutants in the valley (Sapkota and Dhaubhadel, 2002). Others investigated the aerosol chemical properties in Nagarkot, at the rim of the Kathmandu valley, and found that the aerosol featured a dominant contribution from carbon, likely from fuel and biomass burning combustion sources in the Kathmandu valley (Carrico et al., 2003). More recent research shows elevated levels of black carbon and organic carbon in Kathmandu urban air (location 27.7° N, 85.3° E), from September 2004 to August 2005 (Adhikary et al., 2007; Ramanathan et al., 2007). It has been estimated that brick-kilns are responsible for about 28% of annual PM_{10} emissions in the valley, almost all of which is concentrated during the winter months (World Bank, 1997). The operation of 125 brick kilns in the Kathmandu valley during the dry months of December to April has evidently contributed to the aerosol pollution including black carbon emission (Dhakal, 2003; Adhikary et al., 2007).

The PM_{10} spikes at night may provide both the large surface area and the reactive soot for HONO formation. By using an integrated HONO formation per unit area of 5.4×10^{14} molecules cm^{-2} (average value of 8.2×10^{13} molecules cm^{-2}–

1×10^{15} molecules cm^{-2}) (Aubin and Abbatt, 2007; Ammann et al., 1998; Kleffmann and Wiesen, 2005; Kirchner et al., 2000) and the average observed particle surface of 6×10^{-5} cm^{-1} during the plume events of 4 February, the HONO formation by this process is found to be (1.3±0.6) ppb and corresponds to a [HONO]/[NO_2] ratio of 13%±6%, which is in good agreement with our observed increase. This calculation indicates that soot may play a role in NO_2-HONO conversion in Kathmandu. However, it should be noted that there is inadequate information about aerosol chemical composition.

3.4 NO_2 – HONO chemical conversion and correlation studies

The contribution of NO to the formation of HONO by reaction (2), as well as the direct emission from vehicles could be ruled out for Kathmandu late at night because of the low NO concentrations. We have shown that the major source of HONO in the nocturnal air in Kathmandu was the NO_2 to HONO chemical conversion through heterogeneous reactions. HONO formation has been found out to be a first order reaction in NO_2 (Finlayson-Pitts et al., 2003; Kleffmann et al., 1998a). It depends on the surface absorbed water, and increases as the reactive surface to air volume ratio increases (Stutz et al., 2004; Trick, 2004). The ratio of reactive surface to air volume is determined by a combination of the aerosol surface, the ground reactive surface and the influence of vertical mixing (Febo et al., 1996; Trick, 2004). Here we investigate reactive surface-to-air volume ratios (S/V), relative humidity, aerosol size and temperature in the nocturnal atmosphere in Kathmandu and their influence on HONO formation.

The correlation of HONO with other pollutants in Fig. 3 indicates either the presence of all the compounds in the same air mass, or a chemical conversion of NO_2 to HONO associated with aerosols. In order to investigate the efficiency of NO_2-HONO chemical conversion without the influence of other processes (i.e. transport), we study the correlation of [HONO]/[NO_2] instead of [HONO] to the other parameters.

3.4.1 Aerosol surface and ground reactive surface

Long path DOAS measurements can provide the information about aerosol surface-to-air volume ratios $\left(\frac{S}{V}\right)_{\text{aerosol}}$ (see Sect. 2). The ground reactive surface area density $\left(\frac{S}{V}\right)_{\text{ground}}$ is defined as the inverse value of the mixing layer height (H^{-1}) (Vogel et al., 2003; Harrison et al., 1996) in this paper. We use average mixing layer heights from Sonic Detection and Ranging (SODAR) measurements (Panday, 2006). The average mixing layer height deceased from 12 p.m. (800 m) until 0 a.m. (120 m), and then remained at a constant 120 m from 0 a.m. to 6 a.m.

The porosity of aerosols and roughness of the ground surface were not considered in this study. The area densities of aerosol surfaces and ground reactive surface might be higher (up to 10 times) (Lammel and Cape, 1996; Andres-Hernandez et al., 1996) than the calculation values from light attenuation and estimation by mixing layer height, respectively.

Figure 6 shows the behaviors of [HONO]/[NO_2], $\left(\frac{S}{V}\right)_{\text{aerosol}}$ and $\left(\frac{S}{V}\right)_{\text{ground}}$ during a selected night. The black line in Fig. 6 is the combination of the two surface area densities. [HONO]/[NO_2] increased after sunset and remained relatively constant after 0 a.m., then decreased after 3 a.m. $\left(\frac{S}{V}\right)_{\text{aerosol}}$ increased quickly after sunset for a short period, and then stayed nearly constant until 3 a.m. $\left(\frac{S}{V}\right)_{\text{aerosol}}$, as well as PM_{10}, dramatically changed after 3 a.m. The change of $\left(\frac{S}{V}\right)_{\text{aerosol}}$ has a positive correlation with [HONO]/[NO_2] around sunset. However, $\left(\frac{S}{V}\right)_{\text{aerosol}}$ has poor correlation (R^2=0.33) to [HONO]/[NO_2] from 5 p.m. to 3 a.m., which is in contrast to the observed results in some field measurements elsewhere (Notholt et al., 1992a; Reisinger, 2000). It is interesting that $\left(\frac{S}{V}\right)_{\text{ground}}$ has a good correlation with [HONO]/[NO_2] (R^2=0.93) for the whole night except between 3 a.m. and 6 a.m. (see discussion later). The good correlation between [HONO]/[NO_2] and $\left(\frac{S}{V}\right)_{\text{ground}}$ indicated that the NO_2 heterogeneous reaction on the ground reactive surface was a major source of HONO in Kathmandu atmosphere. Our observation of ground reactive surface as a source of atmospheric nitrous acid

is consistent with other field observations (Harrison and Kitto, 1994; Harrison et al., 1996).

3.4.2 Relative humidity (RH)

The RH dependent HONO formation has been studied in laboratory research (Syomin and Finlayson-Pitts, 2003; Harrison and Collins, 1998) and in field observations (Stutz et al., 2004). The RH in the winter of Kathmandu increased from a sunset value of ~60% to ~100% by 3 a.m. and remained close to 100% during most nights in winter in Kathmandu. Figure 7 (panels A, B) shows the time series of [HONO]/[NO_2] and RH in Kathmandu during the entire observation period. It is clear that high RH accompanied the high [HONO]/[NO_2] value, which suggests its influence on the NO_2-HONO conversion.

Figure 8 shows a linear increase of the average [HONO]/[NO_2] values with RH in the RH range of 60% to 96%. However, when RH reached 96%, [HONO]/[NO_2] values decreased. Lammel (1996) had reported that the water coverage of various materials increases dramatically (up to 100 monolayer equivalent water) when RH is over 95%. The surface with a RH of over 95% was classified as "aqueous" surface. Such "aqueous" surface affects the reaction efficiency of NO_2-HONO conversion (Stutz et al., 2004; Lammel, 1999), which is exactly in accordance with our observation.

The HONO formation has been found out to be first order in NO_2, dependent on the surface absorbed water, and increasing with aerosol surface to air volume ratio (Kleffmann et al., 1998b; Sumner et al., 2004; Finlayson-Pitts et al., 2003). The HONO loss is assumed to be first order in HONO on the surface of aerosols or the ground (Syomin and Finlayson-Pitts, 2003). We can thus use Eq. (4) to describe the HONO formation and losses at night in our case, similar to the analysis in previous studies (Finlayson-Pitts and Pitts, 2000; Stutz et al., 2004; Wang et al., 2003):

$$\frac{d[\mathrm{HONO}]}{dt} = \gamma_{\mathrm{NO_2}} \times \frac{\bar{v}_{\mathrm{NO_2}}}{4} \times \frac{S}{V} \times [\mathrm{NO_2}] - \gamma_{\mathrm{HONO}} \times \frac{\bar{v}_{\mathrm{HONO}}}{4} \times \frac{S}{V} \times [\mathrm{HONO}] \quad (4)$$

γ_{NO_2} and γ_{HONO} are HONO formation and destruction reaction probabilities depending on the surface properties, relative humidity, and possibly the particle size and the particle shape (for HONO formation through aerosol reaction). As discussed earlier, S/V is determined by the aerosol surface, the ground reactive surface and the influence of vertical mixing. $\bar{v}_{NO_2}$ and $\bar{v}_{HONO}$ are mean molecular velocities of NO_2 and HONO. When [HONO] reaches the pseudo steady state (PSS), the ratios of [HONO] to [NO_2] is determined by

$$\left(\frac{[HONO]}{[NO_2]}\right)_{PSS} = \frac{\gamma_{NO_2} \times \bar{v}_{NO_2}}{\gamma_{HONO} \times \bar{v}_{HONO}} \quad (5)$$

Since the mean velocities of NO_2 and HONO only differ by 2%, Eq. (5) can be simplified as:

$$\left(\frac{[HONO]}{[NO_2]}\right)_{PSS} = \frac{\gamma_{NO_2}}{\gamma_{HONO}} \quad (6)$$

If our observed HONO in Kathmandu air reached the pseudo steady state, the value of [HONO]/[NO_2] should be determined by the value of γ_{NO_2} and γ_{HONO} at certain RH. The values of the reaction probabilities, γ_{NO_2} and γ_{HONO}, were reported to be in the ranges of 2×10^{-4}–1.5×10^{-3} and 4×10^{-4}–15×10^{-2} (Harrison and Collins, 1998; Bongartz et al., 1994; Msibi et al., 1994; Mertes and Wahner, 1995; Lee and Tang, 1988; Ponche et al., 1993; Kirchner et al., 1990). For example, Harrison and Collins (1998) had reported the γ_{NO_2} and γ_{HONO} values of $5.4\pm0.3\times10^{-4}$ and $2.8\pm0.6\times10^{-3}$ on ammonium sulphate particles at a RH of 85%. Based on their results of particles and an assumption of similar uptake coefficients on the ground reactive surface and entire conversion of NO_2 to HONO on the surface, the value of $\left(\frac{[HONO]}{[NO_2]}\right)_{PSS}$ is calculated as ~19±5% at 85% RH. Mertes and Wahner (1995) had reported the mass accommodation coefficient of $\sim2\times10^{-4}$ for NO_2 and $\sim4\times10^{-3}$ for HONO (lower limit) at a RH of ~100%, which gives value of $\left(\frac{[HONO]}{[NO_2]}\right)_{PSS}$ to be ~5%. Those calculations for $\left(\frac{[HONO]}{[NO_2]}\right)_{PSS}$ from previous publications are consistent with our observation.

Syomin and Finlayson-Pitts (2003) suggested that the HONO reaction coefficient (γ_{HONO}) decreases with the increase of RH (0–50%), while Harrison and Collins (1998) reported that γ_{HONO} on aerosols does not show an evident dependence on the RH (50%–85%). In our observations the relative humidity was between 60%–100%. If we use the conclusion from Harrison and Collins (1998) and assume that the HONO formation reached the pseudo steady state at the RH during our observations, the value of γ_{NO_2} has to increase with increasing RH in order to explain the results shown in Fig. 8.

When RH reaches 100%, the number of water monolayers on the various surface (stone, soil, and vegetation) increases very rapidly (Lammel, 1999). Assuming that 10 to 100 monolayers of water accumulated on the aerosol surface in Kathmandu air when RH increases from 96% to 100% (Lammel, 1999), based on an average thickness of a monolayer of ~0.25 nm (Miranda et al., 1998; Israelachvili and Pashley, 1983; Antognozzi et al., 2001; Opitz et al., 2007), the increase in aerosol diameter should be ~5 nm and 50 nm for 10 and 100 monolayers water uptake on the aerosol. Panel C in Fig. 7 shows that the mean aerosol diameters retrieved from light attenuation increased from 163 nm (RH=96%) to 201 nm (RH=99%). This is in good agreement with our calculation of diameter increase due to water uptake on aerosol surface at RH from 96% to 99%. Furthermore, the increase in diameter leads to an increase in aerosol mass. If the aerosol density is a constant, the aerosol mass should increase by 90% when the mean diameter increases from 163 nm to 201 nm. The Aerosol mass is 132 $\mu g\,m^{-3}$ at a RH of 96% and 259 $\mu g\,m^{-3}$ at a RH of 99%, respectively (Panel C in Fig. 7). This observation of increasing aerosol mass supports the hypothesis of water uptake on aerosol in Kathmandu at night.

The water uptake processes can lead to the fog formation. The fog that usually formed in the early morning in Kathmandu in winter has been reported by many researchers (Kondo et al., 2002; Regmi et al., 2003; Panday, 2006; Yu et al., 2008a). The water uptake processes can take place on the ground surface in addition to the aerosol surface in Kathmandu atmosphere. As many earlier papers reported, water droplets

(on aerosol or ground) at a RH of over 96% play a role in the HONO sink, leading to lower [HONO]/[NO_2] values, which is in agreement with our observation (Lammel and Perner, 1988; Zhou et al., 2007; He et al., 2006; Acker et al., 2001, 2005; Lammel, 1999). Besides the HONO loss in bulk water on the aerosol and ground surface, the increase of aerosol size (Panel C in Fig. 7) at high RH (>96%) may reduce the NO_2 chemical conversion efficiency to form HONO.

3.4.3 Temperature

Most early laboratory studies of NO_2-HONO conversion on the surface were under constant temperature conditions. However, temperatures during the field observations of nocturnal atmospheric nitrous acid are often lower than laboratory temperatures and decreases after sunset. Figure 7 (Panel D) shows that the average temperature decreased from 288 K to 280 K at the night of Kathmandu. It is therefore necessary to investigate the influence of temperature on NO_2-HONO conversion.

The possible reasons of temperature influence on the NO_2-HONO conversion are:

1. Temperature affects the water uptake on the surface;
2. Temperature influences the solubility or uptake of NO_2 and HONO on the surface;
3. Temperature affects some chemical reactions (i.e. $NO_2+NO_2 \rightleftharpoons N_2O_4$).

The uptake of water on various surfaces is dependent on the RH as well as surface materials; such water uptake studies were performed under constant temperature with a Brunauer, Emmett and Teller (BET) isotherm (Lammel, 1999; Sumner et al., 2004; Gustafsson et al., 2005; Seisel et al., 2004; Schuttlefield et al., 2007).

Previous research shows that the amount of water adsorbed on mineral dust and soot increases with decreasing temperature (Seisel et al., 2005). If this was the case in Kathmandu, the water coverage on the surface should increase with decreasing temperature.

The water adsorption on the aerosol and ground surface can be determined by BET isotherm (Eq. 7) (Adamson and Gast, 1997),

$$\textit{fractional coverage} = \frac{c_B \mathrm{RH}}{(1 - \mathrm{RH})[1 + (c_B - 1)\mathrm{RH}]} \quad (7)$$

where

$$c_B = e^{-\left[\frac{\Delta H_1^0 - \Delta H_2^0}{RT}\right]},$$

RH is relative humidity.

ΔH_1^0 and ΔH_2^0 are the standard enthalpy of adsorption of water on the first layer and subsequent layers, respectively; R is the gas constant; T is the temperature in K.

In Eq. (7), c_B, which reflects the strength of the interaction of water vapour with the surface, determines the shape of the isotherm.

For the non-polar surface (c_B equal to 0.1, the interaction between the water and surface is weak and the isotherm is classified as Type III – Adamson and Gast, 1997), the water uptake for increasing RH (60–100%) is hardly influenced by temperature changes at night of Kathmandu (from 288 to 280 K). Similarly, the temperature influence of water uptake for polar surface (c_B equal to 20, the isotherm classified as Type II – Adamson and Gast, 1997; Gregg and Sing, 1982) is very small. The temperature influence of water uptake on the aerosol surface and ground surface during our observation periods is, therefore, not important.

The solubility of HONO in the water films of the atmospheric aerosol and ground surface is determined by Henry's law and the acidity of liquid phase due to rapidly established equilibrium of $HNO_2 + H_2O \rightleftharpoons NO_2^- + H_3O^+$. The Henry constants of NO_2 and HONO are temperature dependant parameters and increase by 28% and 60% with the temperature decrease from 288 K to 280 K (Mertes and Wahner, 1995). Considering the temperature dependence of the dissociation constant of nitrous acid and assuming neutral conditions (pH=7), the solubility of nitrous acid increases by 35% with the decreasing temperature from 288 K to 280 K. Moreover, model calculations have shown

that the HONO mass accommodation coefficient increasing by about an order of magnitude from room temperature to 245 K (Davidovits et al., 1991), which exceeds the experimental results reported by Bongartz et al (1994). This increase of solubility or mass accommodation of HONO may affect the NO_2-HONO chemical conversion. However, due to lack of detailed information about temperature dependent NO_2 and HONO mass accommodations and the acidity information of liquid phase on the aerosol and ground surface in Kathmandu, the importance of temperature influence on the HONO formation through NO_2 heterogeneous reactions on the aerosol and ground surface is not clear in this study.

A mechanism of HONO formation through NO_2 hydrolysis with N_2O_4 adsorbed on water surface has been proposed by earlier laboratory studies (Finlayson-Pitts et al., 2003; Mertes and Wahner, 1995; Ramazan et al., 2006). $NO_2+NO_2 \rightleftharpoons N_2O_4$ is a temperature dependent equilibrium that shifts towards the dimmer, N_2O_4, with decreasing temperature. However, since the NO_2 levels during field observations are much lower than those of laboratory studies, extrapolating this mechanism to the atmospheric HONO formation requires more considerations.

4 Conclusions

Measurements of NO_x, HONO, PM_{10}, surface density, and meteorological parameters in the winter in Kathmandu were presented. To our knowledge, this was the first time that HONO was measured in South Asia.

Very high values of chemically formed HONO to NO_2 ratios were found (up to 30%), which is higher than any other previous atmospheric observations that we are aware of. Our observation showed unusual heterogeneous conversion of NO_2 to HONO during the aerosol plume spikes at the middle night of Kathmandu.

It is believed that direct emission and nitric oxide involved heterogeneous reactions are not the major source of HONO in Kathmandu's nocturnal atmosphere. NO_2 heterogeneous chemical processes are responsible for the high and periodic HONO levels

under the conditions of high aerosol pollution burden, strong inversion, and high humidity. Very low mixing layer height provides large reactive surfaces for the HONO formation through NO_2 heterogeneous reaction, which is confirmed by the good correlation of ground reactive surface area density and [HONO]/[NO_2] values.

The high relative humidity found in Kathmandu at night provides efficient water uptake on reactive surfaces. When relative humidity exceeds 96% in the early morning, the water condensed on aerosol and ground to form water droplets, which appeared to be a sink of gaseous nitrous acid.

Acknowledgement. We would also like to thank the management and especially Mr. Rabindra Poudel at the Taragaon Hyatt Regency Hotel in Kathmandu for their exceptional efforts in providing logistical and engineering support throughout the field campaign. We would like to thank Mr. Sherpa of Bouddha for permitting us to install the retroreflectors on the top floor of his house. The field campaign was partially funded through a seed-project grant from the AGS (Alliance for Global Sustainability). Support was also provided by the MIT Joint Program on the Science and Policy of Global Change.

References

Acker, K., Moller, D., Wieprecht, W., Auel, R., Kalass, D., and Tscherwenka, W.: Nitrous and nitric acid measurements inside and outside of clouds at Mt. Brocken, Water Air Soil Poll., 130, 331–336, 2001.

Acker, K., Moller, D., Auel, R., Wieprecht, W., and Kalass, D.: Concentrations of nitrous acid, nitric acid, nitrite and nitrate in the gas and aerosol phase at a site in the emission zone during ESCOMPTE 2001 experiment, Atmos. Res., 74, 507–524, 2005.

Adamson, A. W. and Gast, A. P.: Physical Chemistry of Surfaces, 6th ed., John Wiley & Sons, Inc., New York, 1997.

Adhikary, B., Carmichael, G. R., Tang, Y., Leung, L. R., Qian, Y., Schauer, J. J., Stone, E. A., Ramanathan, V., and Ramana, M. V.: Characterization of the seasonal cycle of south Asian aerosols: A regional-scale modeling analysis, J. Geophys. Res., 112, D22S22, doi:10.1029/2006JD008143, 2007.

Akimoto, H., Takagi, H., and Sakamaki, F.: Photoenhancement of the nitrous acid formation in the surface reaction of nitrogen dioxide and water vapor: extra radical source in smog chamber experiments, Int. J. Chem. Kinet., 19, 539–551, 1987.
Al-Abadleh, H. A. and Grassian, V. H.: Heterogeneous reaction of NO_2 on hexane soot: A Knudsen cell and FT-IR study, J. Phys. Chem. A., 104, 11 926–11 933, 2000.
Alcala-Jornod, C., van den Bergh, H., and Rossi, M. J.: Reactivity of NO_2 and H_2O on soot generated in the laboratory: a diffusion tube study at ambient temperature, Phys. Chem. Chem. Phys., 2, 5584–5593, 2000.
Ammann, M., Kalberer, M., Jost, D. T., Tobler, L., Rossler, E., Piguet, D., Gaggeler, H. W., and Baltensperger, U.: Heterogeneous production of nitrous acid on soot in polluted air masses, Nature, 395, 157–160, 1998.
Andres-Hernandez, M. D., Notholt, J., Hjorth, J., and Schrems, O.: A DOAS study on the origin of nitrous acid at urban and non-urban sites, Atmos. Environ., 30, 175–180, 1996.
Antognozzi, M., Humphris, A. D. L., and Miles, M. J.: Observation of molecular layering in a confined water film and study of the layers viscoelastic properties, Appl. Phys. Lett., 78, 300–302, 2001.
Arens, F., Gutzwiller, L., Baltensperger, U., Gaggeler, H. W., and Ammann, M.: Heterogeneous reaction of NO_2 on diesel soot particles, Environ. Sci. Technol., 35, 2191–2199, 2001.
Arens, F., Gutzwiller, L., Gaggeler, H. W., and Ammann, M.: The reaction of NO_2 with solid anthrarobin (1,2,10-trihydroxy-anthracene), Phys. Chem. Chem. Phys., 4, 3684–3690, 2002.
Ariola, V., D'Alessandro, A., Lucarelli, F., Marcazzan, G., Mazzei, F., Nava, S., Garcia-Orellana, I., Prati, P., Valli, G., Vecchi, R., and Zucchiatti, A.: Elemental characterization of PM_{10}, $PM_{2.5}$ and PM_1 in the town of Genoa (Italy), Chemosphere, 62, 226–232, 2006.
Aubin, D. G. and Abbatt, J. P. D.: Interaction of NO_2 with hydrocarbon soot: Focus on HONO yield, surface modification, and mechanism, J. Phys. Chem. A, 111, 6263–6273, 2007.
Aumont, B., Madronich, S., Ammann, M., Kalberer, M., Baltensperger, U., Hauglustaine, D., and Brocheton, F.: On the NO_2 plus soot reaction in the atmosphere, J. Geophys. Res., 104, 1729–1736, 1999.
Beine, H. J., Amoroso, A., Domin, F., King, M. D., Nardino, M., Ianniello, A., and France, J. L.: Surprisingly small HONO emissions from snow surfaces at Browning Pass, Antarctica, Atmos. Chem. Phys., 6, 2569–2580, 2006, http://www.atmos-chem-phys.net/6/2569/2006/.
Bejan, I., Abd El Aal, Y., Barnes, I., Benter, T., Bohn, B., Wiesen, P., and Kleffmann, J.: The

photolysis of ortho-nitrophenols: a new gas phase source of HONO, Phys. Chem. Chem. Phys., 8, 2028–2035, 2006.
Bongartz, A., Kames, J., Schurathy, U., George, C., Mirabel, P., and Pnoche, J. L.: Experimental determination of HONO mass accommodation coefficients using two different techniques, J. Atmos. Chem., 18, 149–169, 1994.
Box, M. A. and Lo, S. Y.: Approximate determination of aerosol size distributions, J. Appl. Meteorol., 15, 1068–1076, 1976.
Carrico, C. M., Bergin, M. H., Shrestha, A. B., Dibb, J. E., Gomes, L., and Harris, J. M.: The importance of carbon and mineral dust to seasonal aerosol properties in the Nepal Himalaya, Atmos. Environ., 37, 2811–2824, 2003.
Cheng, M. T., Horng, C. L., and Lin, Y. C.: Characteristics of atmospheric aerosol and acidic gases from urban and forest sites in central Taiwan, Bull. Environ. Contamin. Toxicol., 79, 674–677, 2007.
Davidovits, P., Jayne, J. T., Duan, S. X., Worsnop, D. R., Zahniser, M. S., and Kolb, C. E.: Uptake of gas molecules by liquids: a model, J. Phys. Chem., 95, 6337–6340, 1991.
Domine, F. and Shepson, P. B.: Air-snow interactions and atmospheric chemistry, Science, 297, 1506–1510, 2002.
Ehrlich, C., Noll, G., Kalkoff, W. D., Baumbach, G., and Dreiseidler, A.: PM_{10}, $PM_{2.5}$ and $PM_{1.0}$ – Emissions from industrial plants – Results from measurement programmes in Germany, Atmos. Environ., 41, 6236–6254, 2007.
Febo, A., Perrino, C., and Allegrini, I.: Measurement of nitrous acid in Milan, Italy, by DOAS and diffusion denuders, Atmos. Environ., 30, 3599–3609, 1996.
Finlayson-Pitts, B. J. and Pitts Jr., J. N.: Chemistry of the upper and lower atmosphere – theory, experiments, and applications, Academic Press, San Diego, 969 pp., 2000.
Finlayson-Pitts, B. J., Wingen, L. M., Sumner, A. L., Syomin, D., and Ramazan, K. A.: The Heterogeneous hydrolysis of NO_2 in laboratory systems and in outdoor and indoor atmospheres: an integrated mechanism, Phys. Chem. Chem. Phys., 5, 223–242, 2003.
Flentje, H., Dubois, R., Heintzenberg, J., and Karbach, H. J.: Retrieval of aerosol properties from boundary layer extinction measurements with a DOAS system, Geophys. Res. Lett., 24, 2019–2022, 1997.
Geiger, H., Kleffmann, J., and Wiesen, P.: Smog chamber studies on the influence of diesel exhaust on photosmog formation, Atmos. Environ., 36, 1737–1747, 2002.
George, C., Strekowski, R. S., Kleffmann, J., Stemmler, K., and Ammann, M.: Photoenhanced

uptake of gaseous NO_2 on solid-organic compounds: a photochemical source of HONO?, Faraday Discuss., 130, 195–210, 2005.
Gerecke, A., Thielmann, A., Gutzwiller, L., and Rossi, M. J.: The chemical kinetics of HONO formation resulting from heterogeneous interaction of NO_2 with flame soot, Geophys. Res. Lett., 25, 2453–2456, 1998.
Giri, D., Murthy, V. K., Adhikary, P. R., and Khanal, S. N.: Ambient air quality of Kathmandu Valley as reflected by atmospheric particulate matter concentrations (PM_{10}), Int. J. Environ. Sci. Tech., 3, 403–410, 2006.
Gomiscek, B., Hauck, H., Stopper, S., and Preining, O.: Spatial and temporal variations of PM_1, $PM_{2.5}$, PM_{10} and particle number concentration during the AUPHEP-project, Atmos. Environ., 38, 3917–3934, 2004.
Grassian, V. H.: Heterogeneous uptake and reaction of nitrogen oxides and volatile organic compounds on the surface of atmospheric particles including oxides, carbonates, soot and mineral dust: implications for the chemical balance of the troposphere, Int. Rev. Phys. Chem., 20, 467–548, 2001.
Grassian, V. H.: Chemical reactions of nitrogen oxides on the surface of oxide, carbonate, soot and mineral dust particles: implications for the chemical balance of the troposphere, J. Phys. Chem. A., 106, 860–877, 2002.
Gregg, S. J. and Sing, K. S. W.: Adsorption, surface area and porosity, 2nd ed., Academic Press, London, 1982.
Gustafsson, R. J., Orlov, A., Badger, C. L., Griffiths, P. T., Cox, R. A., and Lambert, R. M.: A comprehensive evaluation of water uptake on atmospherically relevant mineral surfaces: DRIFT spectroscopy, thermogravimetric analysis and aerosol growth measurements, Atmos. Chem. Phys., 5, 3415–3421, 2005, http://www.atmos-chem-phys.net/5/3415/2005/.
Gustafsson, R. J., Orlov, A., Griffiths, P. T., Cox, R. A., and Lambert, R. M.: Reduction of NO_2 to nitrous acid on illuminated titanium dioxide aerosol surfaces: implications for photocatalysis and atmospheric chemistry, Chem. Commun., 3936–3938, 2006.
Hao, N., Zhou, B., Chen, D., and Chen, L. M.: Observations of nitrous acid and its relative humidity dependence in Shanghai, J. Environ. Sci., 18, 910–915, 2006.
Harrison, R. M. and Kitto, A.-M. N.: Envidence for a surface source of atmospheric nitrous acid, Atmos. Environ., 28, 1089–1094, 1994.
Harrison, R. M., Peak, J. D., and Collins, G. M.: Tropospheric cycle of nitrous acid, J. Geophys.

Res., 101, 14429–14439, 1996.
Harrison, R. M. and Collins, G. M.: Measurements of reaction coefficients of NO_2 and HONO on aerosol particles, J. Atmos. Chem., 30, 397–406, 1998.
He, Y., Zhou, X. L., Hou, J., Gao, H. L., and Bertman, S. B.: Importance of dew in controlling the air-surface exchange of HONO in rural forested environments, Geophys. Res. Lett., 33, L02813, doi:10.1029/2005GL024348, 2006.
Heland, J., Kleffmann, J., Kurtenbach, R., and Wiesen, P.: A new instrument to measure gaseous nitrous acid (HONO) in the atmosphere, Environ. Sci. Technol., 35, 3207–3212, 2001.
Honrath, R. E., Lu, Y., Peterson, M. C., Dibb, J. E., Arsenault, M. A., Cullen, N. J., and Steffen, K.: Vertical fluxes of NO_x, HONO, and HNO_3 above the snowpack at Summit, Greenland, Atmos. Environ., 36, 2629–2640, 2002.
Hu, M., Zhou, F. M., Shao, K. S., Zhang, Y. H., Tang, X. Y., and Slanina, J.: Diurnal variations of aerosol chemical compositions and related gaseous pollutants in Beijing and Guangzhou, J. Environ. Sci. Heal. A., 37, 479–488, 2002.
Huang, G., Zhou, X. L., Deng, G. H., Qiao, H. C., and Civerolo, K.: Measurements of atmospheric nitrous acid and nitric acid, Atmos. Environ., 36, 2225–2235, 2002.
IPCC: Climate Change 2001: The Scientific Basis: Contributation of Working Group I to the Third Assessment Report of the Intergovernmental Panel on Climate Change, Cambridge University Press, Cambridge, UK, 2001.
Israelachvili, J. N. and Pashley, R. M.: Molecular layering of water at surfaces and origin of repulsive hydration forces, Nature, 306, 249–250, 1983.
Kanda, Y. and Taira, M.: Chemiluminescent method for continuous monitoring of nitrous-acid in ambient air, Anal. Chem., 62, 2084–2087, 1990.
Kang, C. M., Kang, B. W., and Lee, H. S.: Source identification and trends in concentrations of gaseous and fine particulate principal species in Seoul, South Korea, J. Air Waste Manag., 56, 911–921, 2006.
Karagulian, F. and Rossi, M. J.: Heterogeneous chemistry of the NO_3 free radical and N_2O_5 on decane flame soot at ambient temperature: reaction products and kinetics, J. Phys. Chem. A., 111, 1914–1926, 2007.
Kirchner, U., Scheer, V., and Vogt, R.: FTIR spectroscopic investigation of the mechanism and kinetics of the heterogeneous reactions of NO_2 and HNO_3 with soot, J. Phys. Chem. A., 104, 8908–8915, 2000.

Kirchner, W., Welter, F., Bongartz, A., Kames, J., Schweighoefer, S., and Schurath, U.: Trace gas exchange at the air/water interface: measurements of mass accommodation coefficients, J. Atmos. Chem., 10, 427–449, 1990.
Kirchstetter, T. W., Harley, R. A., and Littlejohn, D.: Measurement of nitrous acid in motor vehicle exhaust, Environ. Sci. Technol., 30, 2843–2849, 1996.
Kleffmann, J., Becker, K. H., and Wiesen, P.: Heterogeneous NO_2 conversion processes on acid surfaces: possible atmospheric implications, Atmos. Environ., 32, 2721–2729, 1998a.
Kleffmann, J., Becker, K. H., and Wiesen, P.: Investigation of the heterogeneous NO_2 conversion on perchloric acid surfaces, J. Chem. Soc. Faraday T., 94, 3289–3292, 1998b.
Kleffmann, J., Heland, J., Kurtenbach, R., Lorzer, J., and Wiesen, P.: A new instrument (LOPAP) for the detection of nitrous acid (HONO), Environ. Sci. Poll. Res, 48–54, 2002.
Kleffmann, J. and Wiesen, P.: Heterogeneous conversion of NO_2 and NO on HNO_3 treated soot surfaces: atmospheric implications, Atmos. Chem. Phys., 5, 77–83, 2005, http://www.atmos-chem-phys.net/5/77/2005/.
Kleffmann, J.: Daytime sources of nitrous acid (HONO) in the atmospheric boundary layer, Chem. Phys. Chem., 8, 1137–1144, 2007.
Kondo, A., Shrestha, M., Kaga, A., Inoue, Y., and Sapkota, B.: Comparison of field observation with water tank experiment on air pollution concentration in Katmandu valley, Adv. Air Poll., 11, 493–502, 2002.
Kurtenbach, R., Becker, K. H., Gomes, J. A. G., Kleffmann, J., Lorzer, J. C., Spittler, M., Wiesen, P., Ackermann, R., Geyer, A., and Platt, U.: Investigations of emissions and heterogeneous formation of HONO in a road traffic tunnel, Atmos. Environ., 35, 3385–3394, 2001.
Labban, R., Veranth, J. M., Chow, J. C., Engelbrecht, J. L. P., and Watson, J. G.: Size and geographical variation in PM_1, $PM_{2.5}$ and PM_{10}: source profiles from soils in the western United States, Water Air Soil Poll., 157, 13–31, 2004.
Lahoutifard, N., Ammann, M., Gutzwiller, L., Ervens, B., and George, C.: The impact of multiphase reactions of NO_2 with aromatics: a modelling approach, Atmos. Chem. Phys., 2, 215–226, 2002, http://www.atmos-chem-phys.net/2/215/2002/.
Lammel, G. and Perner, D.: The Atmospheric aerosol as a source of nitrous-acid in the polluted atmosphere, J. Aerosol Sci., 19, 1199–1202, 1988.
Lammel, G. and Cape, J. N.: Nitrous acid and nitrite in the atmosphere, Chem. Soc. Rev., 25,

361–369, 1996.
Lammel, G.: Formation of Nitrous Acid: Parameterization and Comparison with Observations, Max-Planck-Institut für Meteorologie, Hamburg, Germany, 286, 1–36, 1999.
Lee, J. H. and Tang, I. N.: Accommodation coefficient of gaseous NO_2 on water surfaces, Atmos. Environ., 22, 1147–1151, 1988.
Li, C. S. and Lin, C. H.: $PM_1/PM_{2.5}/PM_{10}$ characteristics in the urban atmosphere of Taipei, Aerosol Sci. Tech., 36, 469–473, 2002.
Liao, W., Case, A. T., Mastromarino, J., Tan, D., and Dibb, J. E.: Observations of HONO by laser-induced fluorescence at the South Pole during ANTCI 2003, Geophys. Res. Lett., 33, L09810, doi:09810.01029/02005GL025470, 2006a.
Liao, W., Hecobian, A., Mastromarino, J., and Tan, D.: Development of a photo-fragmentation/laser-induced fluorescence measurement of atmospheric nitrous acid, Atmos. Environ., 40, 17–26, 2006b.
Liu, Y. S., Chen, R., Shen, X. X., and Mao, X. L.: Wintertime indoor air levels of PM_{10}, $PM_{2.5}$ and PM_1 at public places and their contributions to TSP, Environ. Int., 30, 189–197, 2004.
Livingston, J. M. and Russell, P. B.: Retrieval of aerosol size distribution moments from multi-wavelength particulate extinction measurements, J. Geophys. Res., 94, 8425–8433, 1989.
Longfellow, C. A., Ravishankara, A. R., and Hanson, D. R.: Reactive uptake on hydrocarbon soot: focus on NO_2, J. Geophys. Res., 104, 13 833–13 840, 1999.
Matsumoto, M. and Okita, T.: Long term measurements of atmospheric gaseous and aerosol species using an annular denuder system in Nara, Japan, Atmos. Environ., 32, 1419–1425, 1998.
Mertes, S. and Wahner, A.: Uptake of nitrogen-dioxide and nitrous-acid on aqueous surfaces, J. Phys. Chem., 99, 14 000–14 006, 1995.
Miranda, P. B., Xu, L., Shen, Y. R., and Salmeron, M.: Icelike water monolayer adsorbed on mica at room temperature, Phys. Rev. Lett., 81, 5876–5879, 1998.
Msibi, I. M., Li, Y., Shi, J. P., and Harrison, R. M.: Determination of heterogeneous reaction probability using deposition profile measurement in an annular reactor: application to the N_2O_5/H_2O reaction, J. Atmos. Chem., 18, 291–300, 1994.
Nienow, A. M. and Roberts, J. T.: Heterogeneous chemistry of carbon aerosols, Annu. Rev. Phys. Chem., 57, 105–128, 2006.
Notholt, J. and Raes, F.: Test of insitu measurements of atmospheric aerosols and trace gases by long path transmission spectroscopy, J. Aerosol Sci., 21, S193–S196, 1990.

Notholt, J., Hjorth, J., and Raes, F.: Long path field-measurements of aerosol parameters and trace gas concentrations – formation of nitrous-acid during foggy periods, J. Aerosol. Sci., 22, S411–S414, 1991.
Notholt, J., Hjorth, J., and Raes, F.: Formation of HNO_2 on aerosol surfaces during foggy periods in the presence of NO and NO_2, Atmos. Environ., 26, 211–217, 1992a.
Notholt, J., Hjorth, J., Raes, F., and Schrems, O.: Simultaneous long path field-measurements of HNO_2, CH_2O and aerosol, Ber. Bunsen. Phys. Chem., 96, 290–293, 1992b.
Opitz, A., Scherge, M., Ahmed, S. I. U., and Schaefer, J. A.: A comparative investigation of thickness measurements of ultra-thin water films by scanning probe techniques, J. Appl. Phys., 101, 064310, doi:10.1063/1061.2712155, 2007.
Panday, A.: The Diurnal cycle of air pollution in the Kathmandu valley, Nepal, Dept. of Earth, Atmospheric, and Planetary Sciences, Massachusetts Institute of Technology, Cambridge, MA, USA, Page 100 pp., 2006.
Park, S. S., Hong, S. B., Jung, Y. G., and Lee, J. H.: Measurements of PM_{10} aerosol and gas-phase nitrous acid during fall season in a semi-urban atmosphere, Atmos. Environ., 38, 4265–4265, 2004.
Perner, D. and Platt, U.: Detection of nitrous-acid in the atmosphere by differential optical-absorption, Geophys. Res. Lett., 6, 917–920, 1979.
Pitz, M., Cyrys, J., Karg, E., Wiedensohler, A., Wichmann, H.-E., and Heinrich, J.: Variability of apparent particle density of an urban aerosol, Environ. Sci. Technol., 37, 4336–4342, 2003.
Ponche, J. L., George, C., and Mirabel, P.: Mass transfer at the air/water interface: mass accommodation coefficients of SO_2, HNO_3, NO_2 and NH_3, J. Atmos. Chem., 16, 1–21, 1993.
Qin, M., Xie, P. H., Liu, W. Q., Li, A., Dou, K., Fang, W., Liu, H. G., and Zhang, W. J.: Observation of atmospheric nitrous acid with DOAS in Beijing, China, J. Environ. Sci., 18, 69–75, 2006.
Ramanathan, V., Li, F., Ramana, M. V., Praveen, P. S., Kim, D., Corrigan, C. E., Nguyen, H., Stone, E. A., Schauer, J. J., Carmichael, G. R., Adhikary, B., and Yoon, S. C.: Atmospheric brown clouds: hemispherical and regional variations in long-range transport, absorption, and radiative forcing, J. Geophys. Res., 112, D22S21, doi:10.1029/2006JD008124, 2007.
Ramazan, K. A., Wingen, L. M., Miller, Y., Chaban, G. M., Gerber, R. B., Xantheas, S. S., and Finlayson-Pitts, B. J.: New experimental and theoretical approach to the heterogeneous hydrolysis of NO_2: key role of molecular nitric acid and its complexes, J. Phys. Chem. A, 110, 6886–6897, 2006.
Regmi, R. P., Kitada, T., and Kurata, G.: Numerical simulation of late wintertime local flows

in Kathmandu valley, Nepal: Implication for air pollution transport, J. Appl. Meteorol., 42, 389–403, 2003.
Reisinger, A. R.: Observations of HNO_2 in the polluted winter atmosphere: possible heterogeneous production on aerosols, Atmos. Environ., 34, 3865–3874, 2000.
Rohrer, F., Bohn, B., Brauers, T., Brning, D., Johnen, F.-J., Wahner, A., and Kleffmann, J.: Characterisation of the photolytic HONO-source in the atmosphere simulation chamber SAPHIR, Atmos. Chem. Phys., 5, 2189–2201, 2005, http://www.atmos-chem-phys.net/5/2189/2005/.
Sapkota, B. and Dhaubhadel, R.: Atmospheric turbidity over Kathmandu valley, Atmos. Environ., 36, 1249–1257, 2002.
Schuttlefield, J. D., Cox, D., and Grassian, V. H.: An investigation of water uptake on clays minerals using ATR-FTIR spectroscopy coupled with quartz crystal microbalance measurements, J. Geophys. Res., 112, D21303, doi:10.1029/2007JD008973, 2007.
Seinfeld, J. H. and Pandis, S. N.: Atmospheric chemistry and physics: from air pollution to climate change, Wiley & Sons, New York, 250–253, 1998.
Seisel, S., Lian, Y., Keil, T., Trukhin, M. E., and Zellner, R.: Kinetics of the interaction of water vapour with mineral dust and soot surfaces at T =298 K, Phys. Chem. Chem. Phys., 6, 1926–1932, 2004.
Seisel, S., Pashkova, A., Lian, Y., and Zellner, R.: Water uptake on mineral dust and soot: a fundamental view of the hydrophilicity of atmospheric particles?, Faraday Discuss., 130, 437–451, 2005.
Sharma, C. K.: Urban air quality of Kathmandu valley “Kingdom of Nepal”, Atmos. Environ., 31, 2877–2883, 1997.
Sharma, T., Rainey, R. C., Neumann, C. M., Shrestha, I. L., Shahi, K. B., Shakya, A., and Khatri, S.: Roadside particulate levels at 30 locations in the Kathmandu Valley, Nepal, Int. J. Environ. Pollut., 17, 293–305, 2002.
Spindler, G., Muller, K., Bruggemann, E., Gnauk, T., and Herrmann, H.: Long-term size-segregated characterization of PM_{10}, $PM_{2.5}$, and PM_1 at the IfT research station Melpitz downwind of Leipzig (Germany) using high and low-volume filter samplers, Atmos. Environ., 38, 5333–5347, 2004.
Stemmler, K., Ammann, M., Donders, C., Kleffmann, J., and George, C.: Photosensitized reduction of nitrogen dioxide on humic acid as a source of nitrous acid, Nature, 440, 195–198, 2006.

Stemmler, K., Ndour, M., Elshorbany, Y., Kleffmann, J., D'Anna, B., George, C., Bohn, B., and Ammann, M.: Light induced conversion of nitrogen dioxide into nitrous acid on submicron humic acid aerosol, Atmos. Chem. Phys., 7, 4237–4248, 2007, http://www.atmos-chem-phys.net/7/4237/2007/.

Stockwell, W. R. and Calvert, J. G.: The Mechanism of NO_3 and HONO formation in the nighttime chemistry of the urban atmosphere, J. Geophys. Res., 88, 6673–6682, 1983.

Stutz, J., Alicke, B., Ackermann, R., Geyer, A., Wang, S. H., White, A. B., Williams, E. J., Spicer, C. W., and Fast, J. D.: Relative humidity dependence of HONO chemistry in urban areas, J. Geophys. Res., 109, D03307, doi:10.1029/2003JD004135, 2004.

Sumner, A. L., Menke, E. J., Dubowski, Y., Newberg, J. T., Penner, R. M., Hemminger, J. C., Wingen, L. M., Brauers, T., and Finlayson-Pitts, B. J.: The Nature of water on surfaces of laboratory systems and implications for heterogeneous chemistry in the troposphere, Phys. Chem. Chem. Phys., 6, 604–613, 2004.

Syomin, D. A. and Finlayson-Pitts, B. J.: HONO decomposition on borosilicate glass surfaces: implications for environmental chamber studies and field experiments, Phys. Chem. Chem. Phys., 5, 5236–5242, 2003.

Takenaka, N., Terada, H., Oro, Y., Hiroi, M., Yoshikawa, H., Okitsu, K., and Bandow, H.: A new method for the measurement of trace amounts of HONO in the atmosphere using an air-dragged aqua-membrane-type denuder and fluorescence detection, Analyst, 129, 1130–1136, 2004.

Trebs, I., Meixner, F. X., Slanina, J., Otjes, R., Jongejan, P., and Andreae, M. O.: Real-time measurements of ammonia, acidic trace gases and water-soluble inorganic aerosol species at a rural site in the Amazon Basin, Atmos. Chem. Phys., 4, 967–987, 2004, http://www.atmos-chem-phys.net/4/967/2004/.

Trick, S.: Formation of nitrous acid on urban surfaces: a physical chemical perspective, Fakultät für Naturwissenschaften und Mathematik, University of Heidelberg, Heidelberg, p. 290, 2004.

Vallius, M. J., Ruuskanen, J., Mirme, A., and Pekkanen, J.: Concentrations and estimated soot content of PM_1, $PM_{2.5}$, and PM_{10} in a subarctic urban atmosphere, Environ. Sci. Technol., 34, 1919–1925, 2000.

Vecera, Z. and Dasgupta, P. K.: Measurement of ambient nitrous-acid and a reliable calibration source for gaseous nitrous-acid, Environ. Sci. Technol., 25, 255–260, 1991.

Vogel, B., Vogel, H., Kleffmann, J., and Kurtenbach, R.: Measured and simulated vertical pro-

files of nitrous acid – Part II. model simulations and indications for a photolytic source, Atmos. Environ., 37, 2957–2966, 2003.

Wang, S. H., Ackermann, R., Spicer, C. W., Fast, J. D., Schmeling, M., and Stutz, J.: Atmospheric observations of enhanced NO_2-HONO conversion on mineral dust particles, Geophys. Res. Lett., 30, 1595, doi:10.1029/2003GL017014, 2003.

World Bank: Urban air quality management strategy in Asia (URBAIR), Kathmandu valley., Technical paper 378, 100 pp., 1997.

Wormhoudt, J., Herndon, S. C., Yelvington, P. E., Miake-Lye, R. C., and Wey, C.: Nitrogen oxide (NO/NO_2/HONO) emissions measurements in aircraft exhausts, J. Propul. Power, 23, 906–911, 2007.

Yu, Y., Geyer, A., Xie, P. H., Galle, B., Chen, L. M., and Platt, U.: Observations of carbon disulfide by differential optical absorption spectroscopy in Shanghai, Geophys. Res. Lett., 31, L11107, doi:11110.11029/GL019543, 2004.

Yu, Y., Panday, A., Hodson, E., Galle, B., and Prinn R.: Monocyclic aromatic hydrocarbons in Kathmandu during the winter season, Water Air Soil Poll., 191, 71–81, 2008a.

Yu, Y., Ezell, M. J., Zelenyuk, A., Imre, D., Alexander, M. L., Ortega, J., D'Anna, B., Harmon, C. W., Johnson, S. N., and Finlayson-Pitts, B. J.: Photooxidation of α-pinene at high relative humidity in the presence of increasing concentrations of NO_x, Atmos. Environ., 42, 5044–5060, 2008b.

Zhang, J., Wang, T., Chameides, W. L., Cardelino, C., Kwok, J., Blake, D. R., Ding, A., and So, K. L.: Ozone production and hydrocarbon reactivity in Hong Kong, Southern China, Atmos. Chem. Phys., 7, 557–573, 2007, http://www.atmos-chem-phys.net/7/557/2007/.

Zhou, X., Civerolo, K., Dai, H., Huang, G., Schwab, J., and Demerjian, K.: Summertime nitrous acid chemistry in the atmospheric boundary layer at a rural site in New York State, J. Geophys. Res., 107, 4590, doi:10.1029/2001JD001539, 2002.

Zhou, X. L., Beine, H. J., Honrath, R. E., Fuentes, J. D., Simpson, W., Shepson, P. B., and Bottenheim, J. W.: Snowpack photochemical production of HONO: a major source of OH in the Arctic boundary layer in springtime, Geophys. Res. Lett., 28, 4087–4090, 2001.

Zhou, X. L., Huang, G., Civerolo, K., Roychowdhury, U., and Demerjian, K. L.: Summertime observations of HONO, HCHO, and O_3 at the summit of Whiteface Mountain, New York, J. Geophys. Res., 112, D08311, doi:10.1029/2006JD007256, 2007.

Table 1. Pollutants in Kathmandu urban air.

Pollutant	Mean (ppbv)[a]						Minimum (ppbv)[a]	Maximum (ppbv)[a]
	Total	SD	Day[b]	SD	Night[c]	SD		
NO_2	14.14	9.77	8.59	5.65	17.94	10.23	0.692	70.11
NO	3.16	6.41	4.41	7.51	2.17	5.19	0.011	162.72
HONO	1.55	1.57	0.351	0.444	1.736	0.804	0.026	7.45
PM_{10}	0.197	0.153	0.216	0.193	0.182	0.109	0.011	1.27

[a] PM_{10} unit is mg m^{-3}; [b] daytime: 7 a.m.–6 p.m.; [c] nocturnal: 6 p.m.–7 a.m.

Table 2. HONO and NO_2 measurements in Asia.

Location	Month/Year	Type	NO_2/ppb (Mean)	HONO/ppb (Mean)	HONO/NO_2
Hong Kong/Hong Kong (Zhang et al., 2007)	Oct–Dec/2002	urban/suburban		~1–10	
Beijing/China (Qin et al., 2006)	Aug–Sept/2004	urban	5–85	0.4–6.1	2%–10%
Shanghai/China (Hao et al., 2006)	Oct/2004–Jan/2005	urban	5.5–75.4 (24)	0.3–6.8 (1.1)	1%–13%
Beijing/China (Hu et al., 2002)	May, June–July, Sept,Dec/2000	urban		0.8–3.1	
Guangzhou/China (Hu et al., 2002)	July, Nov/2000	urban		1.0–2.7	
Taichung/Taiwan (Cheng et al., 2007)	Oct/2002	urban	(39.8±12)	(2.9±1.4)	
Ren-Ai/Taiwan (Cheng et al., 2007)	Oct/2002	Forest	(7.8±1.4)	(0.2±0.1)	
Seoul/South Korea (Kang et al., 2006)	Apr/2001–Feb/2002	urban		0.5–9.7 (2.8)	
Kwangju/South Korea (Park et al., 2004)	Sept–Nov/2001	Semi-urban	0–90	0.02–3.0	2%–6%
Nara/Japan (Matsumoto and Okita, 1998)	June/1994–May/1995	urban		0.4–1.4 (0.75)	
Tsukuba/Japan (Kanda and Taira, 1990)	Feb/1990	rural	5–15	0.2–0.7	
Kathmandu/Nepal (this work)	Jan–Feb/2003	urban	2.9–51.6 (17.9)[a]	0.15–7.45 (1.7)[a]	1%–30% (9.5%)[a]

[a] Only night data

ACPD
9, 183–223, 2009

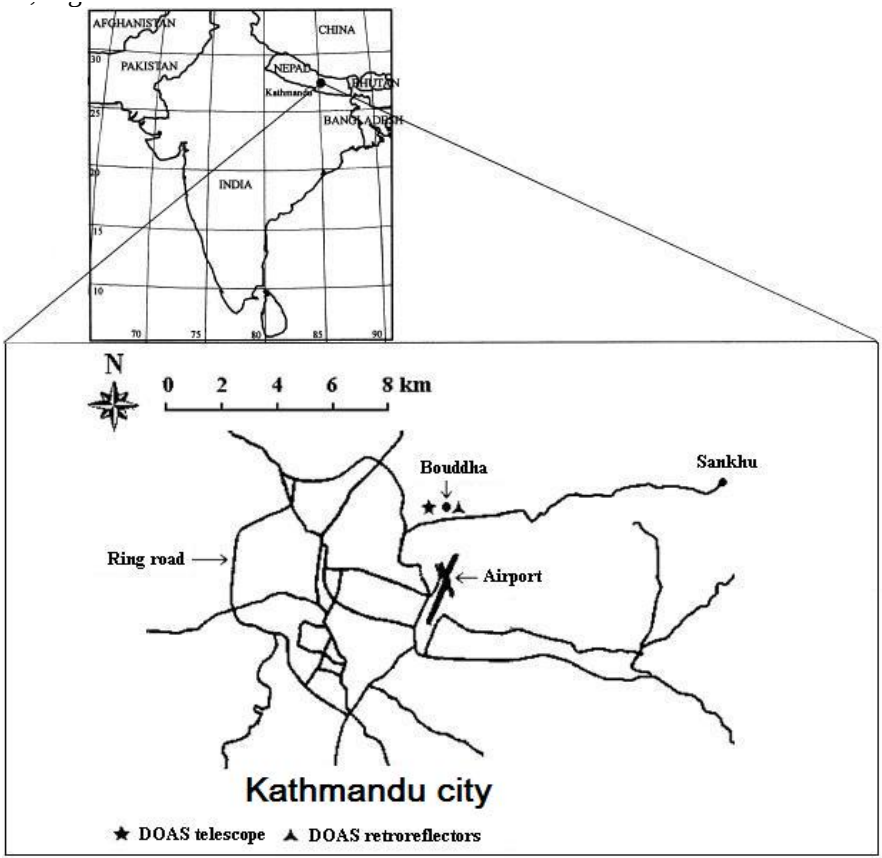

Fig. 1. Map of Kathmandu showing the measurement site.

ACPD
9, 183–223, 2009

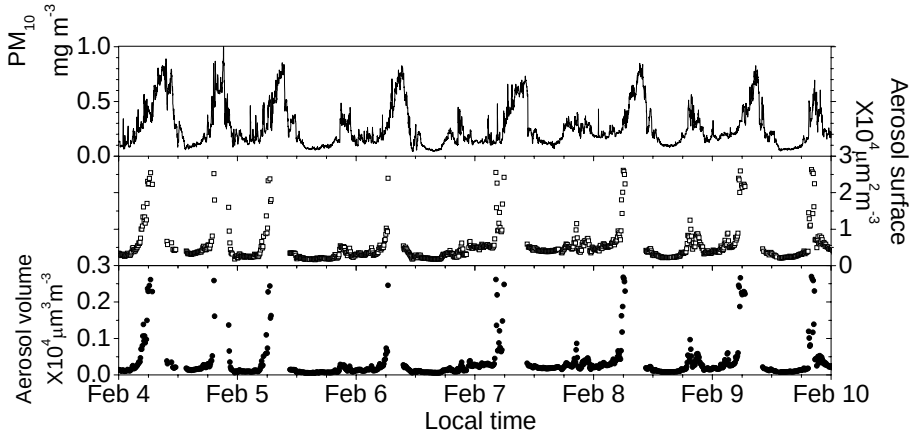

Fig. 2. PM_{10}, aerosol surface and volume measured in Kathmandu, 2003.

ACPD
9, 183–223, 2009

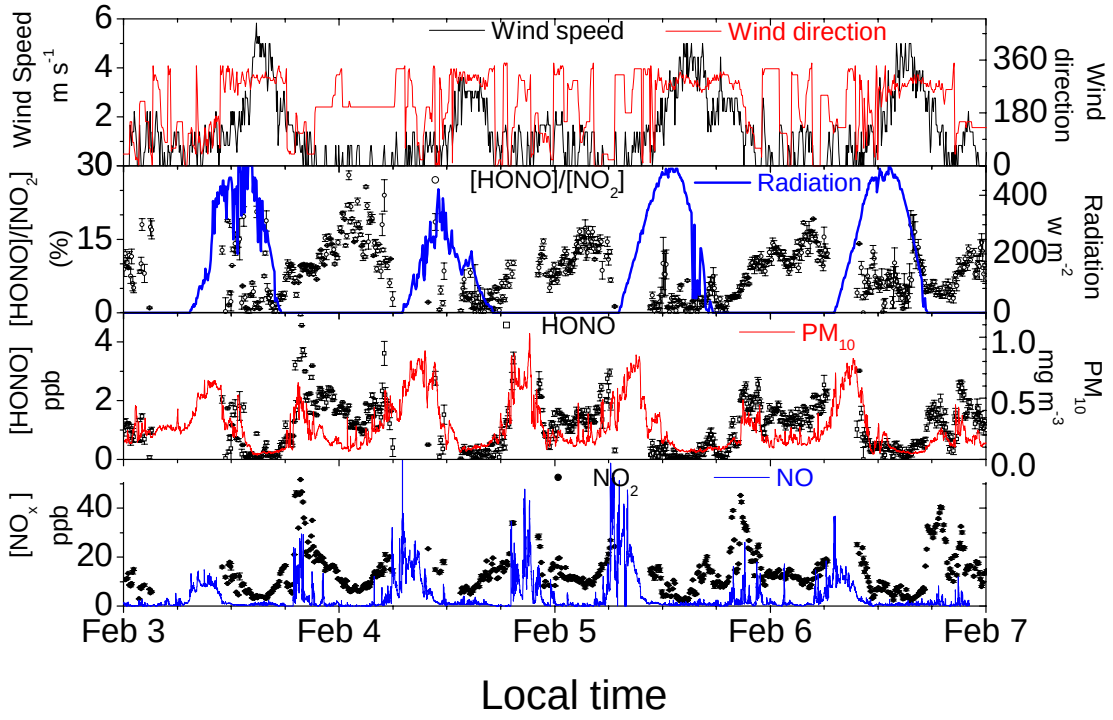

Fig. 3. Behavior of $[NO_2]$, [HONO], $[HONO]/[NO_2]$, PM_{10}, and meteorological parameters (wind speed, wind direction, and solar radiation) during 3–7 February in Kathmandu urban air. The error bars are 1σ standard deviation.

ACPD
9, 183–223, 2009

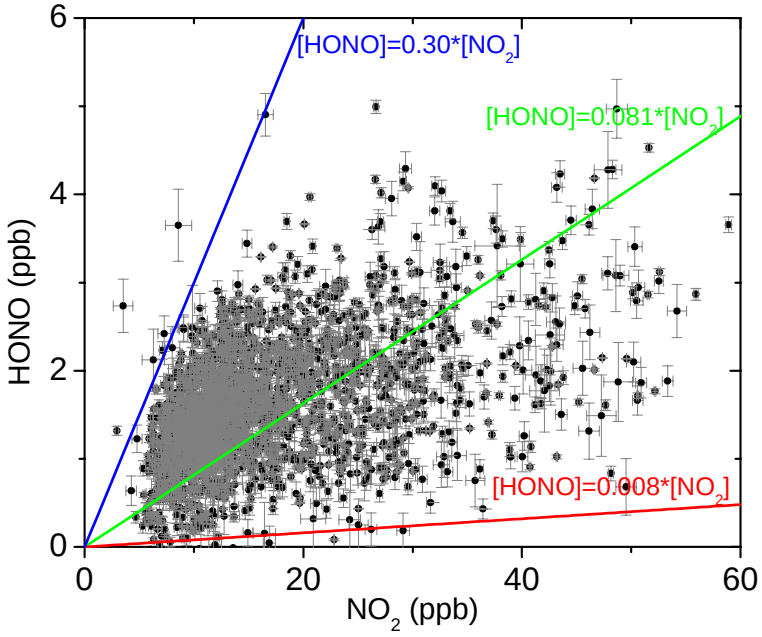

Fig. 4. [HONO] vs. [NO_2] in the nocturnal atmospheric boundary layer at an urban site of Kathmandu. The error bars are 1σ standard deviation.

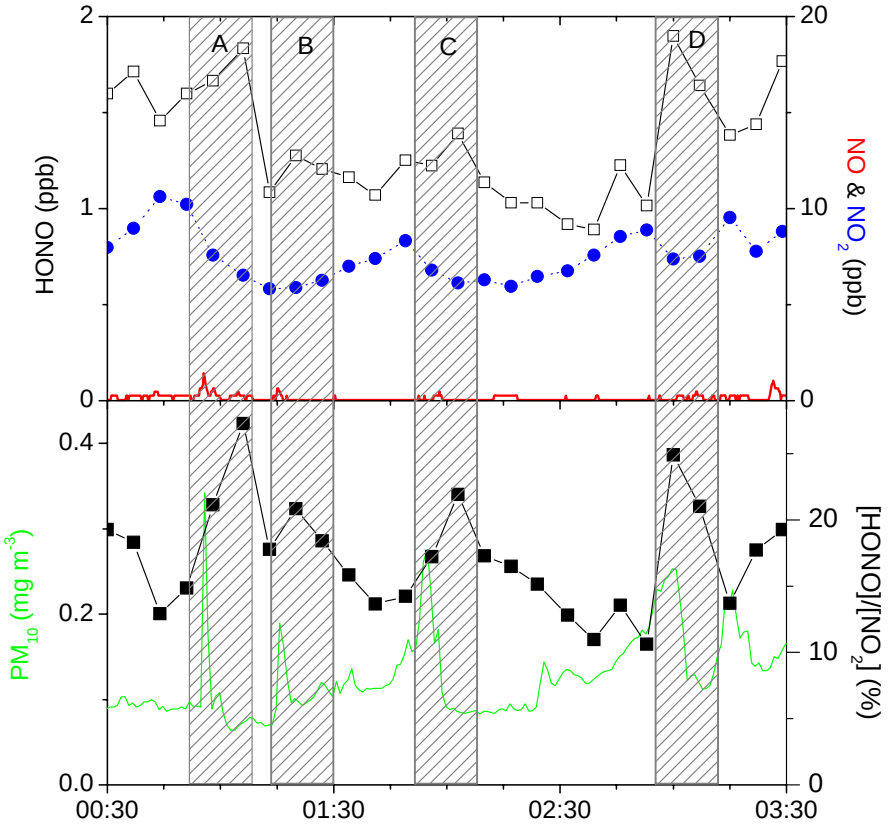

Fig. 5. Observation results indicated the additional NO_2-HONO conversion on the plume particles at the night of 4 February 2003. Top panel: NO_2 (blue dot), NO (red line), HONO (open square); Bottom panel: [HONO]/[NO_2] (black square), PM_{10} (green line).

ACPD
9, 183–223, 2009

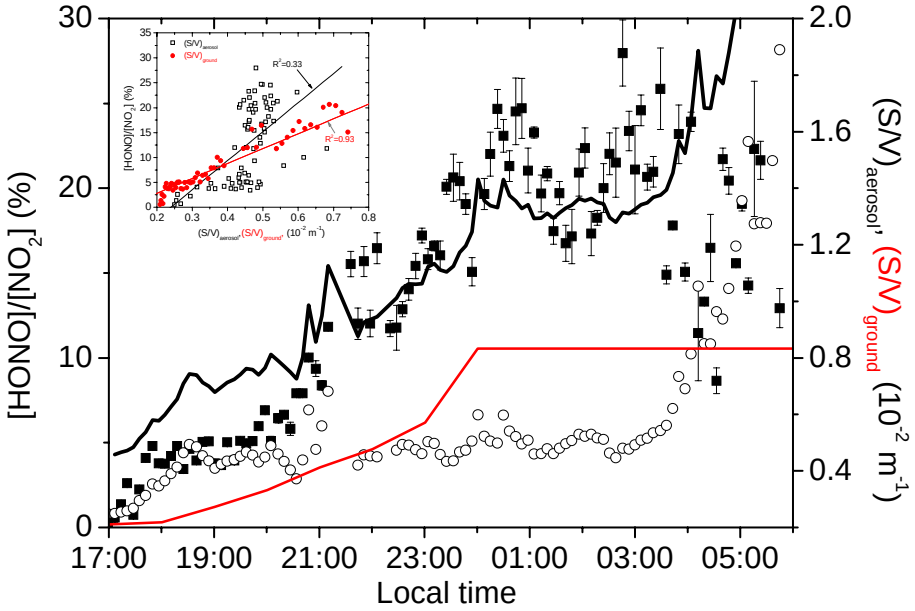

Fig. 6. [HONO]/[NO_2] (square), aerosol surface (open circle), ground reactive surface (red line) and (S/V)aerosol+(S/V)ground (black line) at 21–22 January 2003. Insert: linear regressions of [HONO]/[NO_2] on aerosol surface and ground reactive surface.

ACPD
9, 183–223, 2009

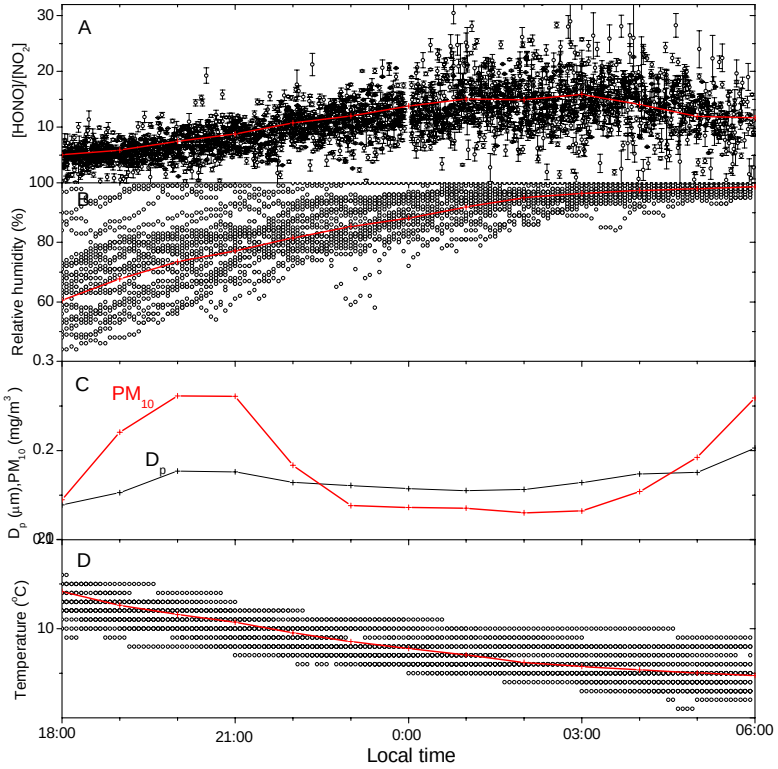

Fig. 7. [HONO]/[NO_2], temperature, relative humidity, PM_{10} and aerosol mean diameters in the nocturnal Kathmandu atmosphere during whole observation period. Line with plus marks are average values.

ACPD
9, 183–223, 2009

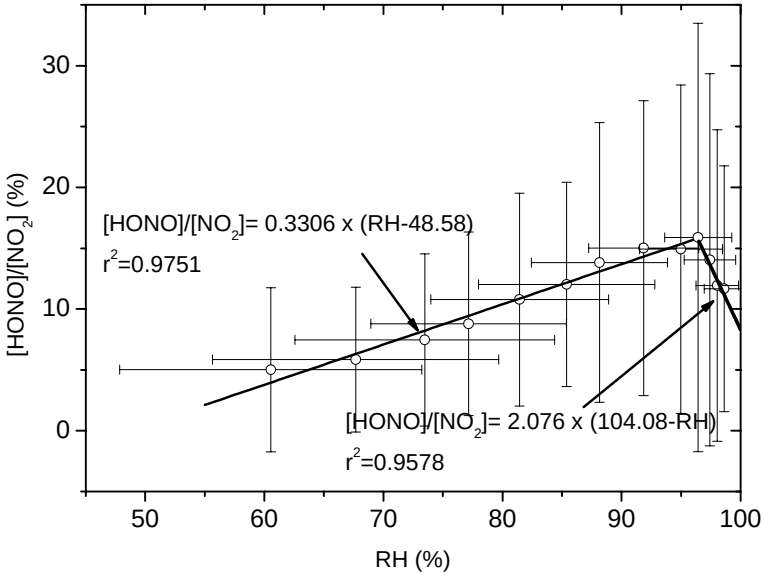

Fig. 8. A scatter plot with error bars shows [HONO]/[NO_2] linear increase at 60–96% RH range and linear decrease at 96–100% RH range. Error bar is standard deviation.

ACPD
9, 183–223, 2009